Available online at www.sciencedirect.com
SCIENCE DIRECT®
Journal of Solid State Chemistry 175 (2003) 27–33
JOURNAL OF SOLID STATE CHEMISTRY
http://elsevier.com/locate/jssc

Alignment of acentric $MoO_3F_3^{3-}$ anions in a polar material: $(Ag_3MoO_3F_3)(Ag_3MoO_4)Cl$

Paul A. Maggard,[a] Tiffany S. Nault,[b] Charlotte L. Stern,[b] and Kenneth R. Poeppelmeier[b,*]

[a] *Department of Chemistry, 2620 Yarbrough Drive, North Carolina State University, Raleigh, NC 27695-8204, USA*
[b] *Department of Chemistry, 2145 Sheridan Road, Northwestern University, Evanston, IL 60208-3113, USA*

Received 24 September 2002; received in revised form 10 January 2003; accepted 18 January 2003

Abstract

$(Ag_3MoO_3F_3)(Ag_3MoO_4)Cl$ was synthesized by hydro(solvato)thermal methods and characterized by single-crystal X-ray diffraction ($P3m1$, No. 156, $Z = 1$, $a = 7.4488(6)$ Å, $c = 5.9190(7)$ Å). The transparent colorless crystals are comprised of chains of distorted *fac*-$MoO_3F_3^{3-}$ octahedra and MoO_4^{2-} tetrahedra anions, as suggested by the formulas $Ag_3MoO_3F_3$ and $Ag_3MoO_4^+$, and are connected through Ag^+ cations in a polar alignment along the *c*-axis. One Cl^- anion per formula unit serves as a charge balance and connects the two types of chains in a staggered fashion, offset by $\sim\frac{1}{2}\times c$. In MoO_4^{2-}, the Mo atom displaces towards a single oxide vertex, and in $MoO_3F_3^{3-}$, the Mo displaces towards the three oxide ligands. The ordered oxide–fluoride ligands on the $MoO_3F_3^{3-}$ anion is important to prevent local inversion centers, while the polar organization is directed by the Cl^- anion and interchain dipole–dipole interactions. The dipole moments of $MoO_3F_3^{3-}$ and MoO_4^{2-} align in the negative *c*-axis direction, to give a polar structure with no cancellation of the individual moments. The direction and magnitude of the dipole moments for $MoO_3F_3^{3-}$ and MoO_4^{2-} were calculated from bond valence analyses and are 6.1 and 1.9 debye (10^{-18} esu cm) respectively, compared to 4.4 debye for polar NbO_6 octahedra in $LiNbO_3$, and 4.5 debye for polar TiO_6 octahedra in $KTiOPO_4$ (KTP).

Keywords: Polar compound; Dipole moment calculation; Metal oxyfluoride anions

1. Introduction

The synthesis of polar materials, one subcategory of the noncentrosymmetric symmetries [1], has been noted increasingly in the literature as a significant goal, or achievement, for the observation of physical properties such as pyroelectricity, ferroelectricity, piezoelectricity, or second harmonic generation (SHG) in a compound. For a material to exhibit one of the two former properties, polar symmetries (crystal classes 1, 2, 3, 4, 6, *m*, *mm*2, 3*m*, 4*mm*, 6*mm*) are a necessary condition, and for the latter two properties, polar symmetry is sufficient, but not necessary [2]. However, symmetry restrictions do not place a limitation on the variety of chemical components or synthetic pathways a chemist could utilize, and several bottom-up approaches for building polar structures have been described. The list of current synthetic strategies includes utilizing molecular host frameworks (guanidinium sulfate sheets, *mm*2) [3], the topology of a metal-organic coordination network (bis(nicotinato)zinc, *mm*2) [4], the packing of chemical species with active lone-pairs (iodate, *mm*2 in $RbMoO_3(IO_3)$, or tellurite, *mm*2 in Te_2SeO_7) [5,6], or with an inherently polar anion (dichromate, *mm*2 in $Cu(py)_4Cr_2O_7$) [7], or an inherently polar ligand arrangement (metal oxide-fluorides, $MoO_3F_3^{3-}$, 3*m* in $(Ag_3MoO_3F_3)(Ag_3MoO_4)Cl$ here).

The electrostatic dipole–dipole interaction is a common structure-directing feature, regardless of whether the polar chemical species are molecules, layers, or networks. Near-neighbor dipole–dipole interactions, either repulsive (+/+, −/−) or attractive (+/−), will determine whether individual polar units combine to form a polar or nonpolar structure (see discussion). These structures can be topologically compared by analyzing the packing and electrostatic interaction of constituent dipole moments. The problem is that while the direction of the *net* dipole moment is usually known (i.e., because it is restricted to lie on a particular

*Corresponding author.
E-mail address: krp@northwestern.edu (K.R. Poeppelmeier).

0022-4596/03/$ - see front matter © 2003 Elsevier Science (USA). All rights reserved.
doi:10.1016/S0022-4596(03)00090-2

symmetry element of a space group, except in noncentrosymmetric $P1$), the individual, atomic, dipole moments may point in any direction, and these typically are ignored. For example, in $Zn(pyz)(H_2O)_2MoO_2F_4$ [8], helical chains propagate down a 3_1 screw axis, which is the allowed direction of a net dipole moment, and yet the individual dipole moments of polar $MoO_2F_4^{2-}$ octahedra point perpendicular to the rotation axis. Of equal importance is how much the neighboring dipoles cancel, for the reason that the 'additive' behavior of dipole moments has a significant effect on second harmonic generation [6,9]. In multicomponent materials, the problem is also to know which chemical species (metal ions, organics, polyatomic ions, or H_2O) imparts the polarity sense.

To impart a polarity sense in a material, our strategy is to utilize polar metal oxide–fluoride octahedra. The oxide-fluoride anions, such as (V, Nb or Ta)OF_5^{2-} and (Mo or W)$O_2F_4^{2-}$, mimic and enhance the polar intra-octahedral structural distortions present in the technologically useful $LiNbO_3$ and $KTiOPO_4$ (KTP) materials [10,11]. However, the first challenge for us to synthesize a polar solid was to prevent oxide-fluoride ligand disorder around the transition metal, and the next, was to prevent the dipole moments of separate octahedra from cancelling each other. The former obstacle, ordering, has been overcome for all five above anions, and lead to an analysis of their intra-octahedral distortions [12]. However, research on the $MoO_3F_3^{3-}$ anion had not, until now, yielded an ordered oxide-fluoride or polar structure. The earliest reported compound to have this anion was synthesized by Pauling, $(NH_4)_3MoO_3F_3$, [13] and others followed with $CsMMoO_3F_3$ (M = Ni, Zn, Mn) [14], $AMoO_3F_3$ (A = Na, K) [15,16], $K_2NaMoO_3F_3$ [17], and $Rb_2KMoO_3F_3$ [18]. Despite the fact these solids were much studied for their ferroelectric–ferroelastic phase transitions, all are reported to have disordered oxide-fluoride ligands on the $MoO_3F_3^{3-}$ anion. (See note added in proof.) For the ferroelectric solids, no complete structure refinement was reported beyond a determination of the space group ($P2_1$, polar and chiral), and the local ligand configuration could be either *fac* or *mer*. We describe herein the *fac*-$MoO_3F_3^{3-}$ anion, together with the MoO_4^{2-} anion, in the polar $(Ag_3MoO_3F_3)(Ag_3MoO_4)Cl$ compound. Dipole moments on the anions have been calculated and illustrates a mechanism for oxide–fluoride ordering, and which also allows a comparison to the dipole moments of other materials, such as $LiNbO_3$ and KTP.

2. Experimental

2.1. Caution

Hydrofluoric acid is toxic and corrosive!

2.1.1. Materials

Ag_2O (99%, Aldrich), MoO_3 (99.9995%, Alfa AESAR), 4-hydroxypyridine (95%, Aldrich), HF (aqueous, 49%, Aldrich), and HCl (aqueous, 37.6%, Fisher Scientific) were used as received. Reagent amounts of deionized water were also used in the synthesis.

2.1.2. Synthesis

$(Ag_3MoO_3F_3)(Ag_3MoO_4)Cl$ was synthesized by adding 3.20×10^{-1} g (2.22×10^{-3} mol) of Ag_2O, 7.73×10^{-1} g (3.33×10^{-3} mol) of MoO_3, 1.06×10^{-1} g (1.11×10^{-3} mol) of 4-hydroxypyridine, 7.88×10^{-1} g (2.22×10^{-2} mol) of 49% aqueous HF, and 1.38×10^{-2} g (5.56×10^{-4} mol) of 37.6% aqueous HCl to an FEP Teflon pouch. The pouch was heat sealed, placed inside a 125 mL autoclave (Parr), and backfilled with ~42 mL deionized H_2O before closing. The autoclave was heated inside a furnace to 150°C for 24 h and slowly cooled to room temperature at 6°C/h. Transparent crystals of $(Ag_3MoO_3F_3)(Ag_3MoO_4)Cl$ were recovered by filtration in ~50% yield based on Ag, with the remaining amount left in solution. The powder pattern of the solid product revealed 100% of the target compound. Higher concentrations of HCl precipitated AgCl, and larger amounts of HF or H_2O lowered the yield of $(Ag_3MoO_3F_3)(Ag_3MoO_4)Cl$. 4-hydroxypyridine remains in solution but is necessary for the crystallization of the target phase, and may be substituted for with pyridine or 4-methylpyridine, while reactions using 2-chloropyridine or 3-chloropyridine give alternate products.

$(Ag_3MoO_3F_3)(Ag_3MoO_4)Cl$ was first obtained via a hydrothermal reaction loaded with Ag_2O, MoO_3, 4-hydroxypyridine, HF and H_2O in a 2:2:5:30:4 molar ratio (1.7 g total), which was heated to 150°C for 24 h and slowly cooled to room temperature for 6°C/h. The presence of the Cl^- ion was established by EDS measurements, and originated from impure Ag_2O starting material. Subsequent reactions, utilizing HCl as the Cl^- ion source, determined the optimum reaction conditions above.

2.1.3. Crystallographic determination

Single crystals of $(Ag_3MoO_3F_3)(Ag_3MoO_4)Cl$ were colorless, transparent, and exhibited a hexagonal platelet morphology. Several crystals were examined under an optical microscope equipped with cross polarizers, and the best selected for data collection on a Bruker CCD diffractometer operating at 153 K. The unit cell obtained was trigonal with $a = 7.4488(6)$ Å and $c = 5.9190(7)$ Å. One sphere of reflections $(\pm h, \pm k, \pm l)$ was collected and processed with SAINTPLUS [19] to $2\theta = 56^\circ$ to give 2654 reflections, of which 563 were unique and $I > 2\sigma_I$. The structure was solved and refined using SHELXTL [20] in the trigonal space group $P3m1$ (No. 156) and checked for additional symmetry elements

using the program PLATON [21]. Floating origin restraints [22], to prevent structure drifting along the polar *c*-axis, were generated automatically by SHELX-97 (which does not require fixing the *z*-coordinate of a single atom) [23]. For comparison, the *z*-coordinate of Ag1 was fixed and the least-squares refinement gave statistically identical results. Final anisotropic structure refinement converged at $R_1/wR_2 = 0.024/0.060$, with a data:variable ratio of ~13:1. The Flack parameter [24,25] was refined and converged at 0.47(7), which indicated the crystal was racemically (inversion) twinned at an approximately 50% ratio, i.e., individual twin domains had dipole moments oriented either "+" or "−" along the *c*-axis. Some data collection and refinement parameters, as well as selected atomic coordinates and isotropic-equivalent displacement parameters, are given in Tables 1 and 2. Complete data collection, refinement and anisotropic displacement parameters, and near-neighbor interatomic distances are available in the Supporting Information.

2.1.4. Spectroscopic measurements

Mid-infrared (400–4000 cm^{-1}) spectra were collected on $(Ag_3MoO_3F_3)(Ag_3MoO_4)Cl$ using a Bio-Rad FTS-60 FTIR spectrometer operating at a resolution of 2 cm^{-1}. The sample was ground and pelletized with dried KBr, transferred to the FTIR spectrometer, and evacuated for 2–5 min before spectrum acquisition.

2.1.5. Magnetic susceptibility

Magnetization on a polycrystalline sample of $(Ag_3MoO_3F_3)(Ag_3MoO_4)Cl$ was measured from 5 to 300 K at a field of 1-kG with a Quantum Design Corp. MPMS SQUID susceptometer. The data were corrected for diamagnetism of both the sample holder and atomic cores.

2.1.6. Nonlinear optical measurements

Powder SHG measurements were performed on a modified Kurtz-NLO system using 1064 nm light [26]. A detailed description of this methodology has been published [6].

Table 1
Selected crystal and refinement data for $(Ag_3MoO_3F_3)(Ag_3MoO_4)Cl$

Empirical formula	$Ag_6Mo_2ClO_7F_3$
f_w	1043.55
Space group, *Z*	*P*3*m*1 (No. 156), 1
T	153(2)
a	7.4488(6)
c	5.9190(7)
V	284.41(5)
μ (Mo*K*α), mm^{-1}	12.524
d_{calc}, $g\,cm^{-3}$	6.09
Flack parameter	0.47(7)
Data/restraints/parameters	565/1/45
final R_1, wR_2[a] $[I > 2\sigma(I)]$	0.024, 0.074

[a] $R_1 = \sum||F_o|-|F_c||/\sum|F_o|$; $wR_2 = \{\sum[w(F_o^2-F_c^2)^2]/\sum[w(F_o^2)^2]\}^{1/2}$, $w = \sigma_F^{-2}$.

3. Results and discussion

3.1. Structural description

The crystal structure of $(Ag_3MoO_3)(Ag_3MoO_4)Cl$, viewed down ~[110] (*c*-axis is vertical), is illustrated in Fig. 1 with symmetry inequivalent atoms and bond distances marked in Å. The compound is comprised of two distinct chains, one with slightly distorted MoO_4^{2-} tetrahedra and the other with highly distorted $MoO_3F_3^{3-}$ octahedra. The octahedral and tetrahedral anions of each chain are bonded from both above and below to three Ag^+ atoms, in a 1:1 repeating fashion, along the length of the polar chain to give the $Ag_3MoO_3F_3$ and $Ag_3MoO_4^+$ chain compositions. The anions of each chain are offset from each other by $\sim\frac{1}{2}\times c$ as a consequence of their coordination to the Cl^- ion, shown along the *c*-axis with the unit cell in Fig. 2. Each Cl^- ion bonds to three Ag atoms on the $Ag_3MoO_4^+$ chains above ($\frac{1}{4}c$), and to three Ag atoms on the $Ag_3MoO_3F_3$

Table 2
Selected atomic coordinates and equivalent isotropic displacement parameters ($Å^2 \times 10^3$) for $(Ag_3MoO_3F_3)(Ag_3MoO_4)Cl$

Atom	Wyck. position	*x*	*y*	*z*[a]	*U*(eq)[b]
Ag1	3*d*	0.82580(6)	0.6516(1)	0.19300(8)	0.0128(3)
Ag2	3*d*	0.49398(5)	0.9880(1)	0.7272(1)	0.0149(3)
Mo1	1*b*	0.3333	0.6667	0.2369(3)	0.0086(4)
Mo2	1*a*	0	0	0.6866(2)	0.0092(4)
Cl	1*c*	0.6667	0.3333	0.4935(7)	0.0142(8)
O1	3*d*	0.4605(5)	0.921(1)	0.125(1)	0.014(1)
O2	3*d*	0.246(1)	0.1230(5)	0.813(1)	0.016(1)
O3	1*b*	0.3333	0.6667	0.539(2)	0.012(2)
F	3*d*	0.1164(3)	0.2329(7)	0.4429(9)	0.0136(9)

[a] *z* coordinates on the polar axis have been least-squares restrained according to [22], the method utilized in SHELX-97 (see text) [23].
[b] *U*(eq) is defined as one-third of the trace of the orthogonalized U_{ij} tensor.

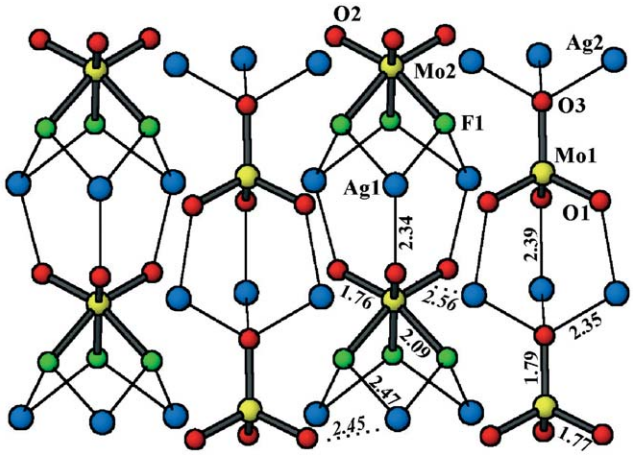

Fig. 1. The polar metal oxide-fluoride chains in $(Ag_3MoO_3F_3)(Ag_3MoO_4)Cl$, with symmetry unique atoms labeled. A 3-fold rotation axis passes vertically down the center of each chain. Distances are marked in Å.

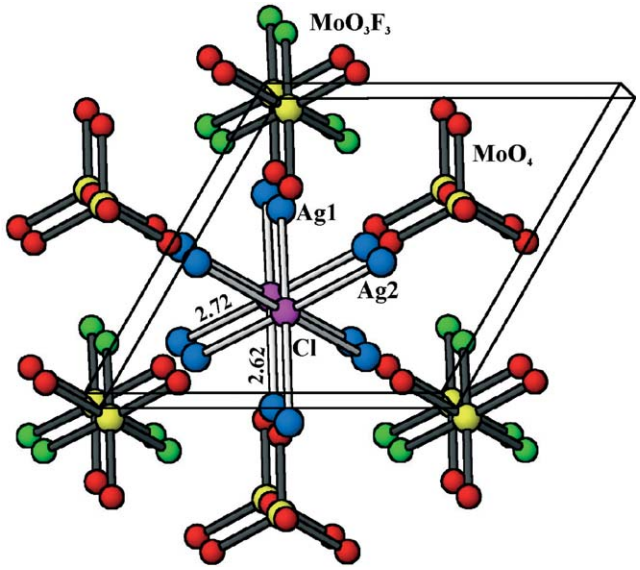

Fig. 2. The hexagonal unit cell of $(Ag_3MoO_3F_3)(Ag_3MoO_4)Cl$, with the $MoO_3F_3^{3-}$ and MoO_4^{2-} anions projected down the *c*-axis. Selected Ag–Cl distances are marked in Å. The octahedral Cl^- environment is comprised of three Ag1 and three Ag2 atoms, from the separate MoO_4^{2-} and $MoO_3F_3^{3-}$ chains.

chains below ($\frac{1}{4}c$), and offsets the chains. Halide ions, such as Cl^-, have been cited as templates in the structures of lanthanum hydroxo complexes recently [27], and here, also has charge-compensating and beneficial packing effects (described below). As a consequence, both chains pack into a hexagonal lattice, space group $P3m1$, with $MoO_3F_3^{3-}$ at $z = 0.6866(2)$, MoO_4^{2-} at $z = 0.2369(3)$, and Cl^- approximately halfway between them on the *c*-axis, at $z = 0.4935(7)$.

Distances and angles around the local Mo environments, listed in Table 3, show significant polar distortions for the MoO_4^{2-} and $MoO_3F_3^{3-}$ polyhedra. A three-fold rotation passes down the middle of the $Ag_3MoO_4^+$ and $Ag_3MoO_3F_3$ chains, and the intra-polyhedral distortions are confined to this rotation axis as well. The MoO_4^{2-} distorted tetrahedron has three symmetry-equivalent oxygen atoms on one face, Mo1–O1 at 1.769(6) Å ($\times 3$) (arbitrarily designated as the base), and one symmetry inequivalent vertex at a slightly longer distance, Mo1–O3 at 1.79(1) Å. Angles around the base of the distorted tetrahedron, O1–Mo1–O1 are slightly compressed at 106.9(2)° and those to the inequivalent vertex, O1–Mo1–O3, are slightly expanded at 111.9(2)°. Owing to the mixed oxide–fluoride ligands, the $MoO_3F_3^{3-}$ octahedron shows greater distortion. Mo2 is coordinated, in a *fac* configuration, by three symmetry equivalent oxygen atoms, Mo2–O2 at 1.755(6) Å ($\times 3$), and also by three symmetry equivalent fluorine atoms, Mo2–F at 2.083(5) Å ($\times 3$). Angles around the oxygen face of the distorted octahedron are very expanded, O2–Mo2–O2 at 103.1(3)°, compared to those around the fluoride face, F–Mo2–F at 77.3(2)°. The smaller fluoride radii accounts for the more compressed angles, compared to the oxide ligands. The ideal point group for the *fac*-configuration of $MoO_3F_3^{3-}$ is $C3v$, which is conserved here in the crystal class $3m$, the only polar crystal class that supports the $C3v$ point group.

The Mo anions are connected by two types of Ag atoms into chains, Ag2 with MoO_4^{2-} and Ag1 with $MoO_3F_3^{3-}$, Fig. 1. Each Ag2 atom bonds once to an oxygen vertex on the base of an MoO_4^{2-} tetrahedron above, Ag2–O1 at 2.395(7) Å, and also to the upper vertex of a tetrahedron below, Ag2–O3 at 2.353(5) Å ($\times 3$). In the chain comprised of $MoO_3F_3^{3-}$ anions, each Ag1 bonds twice to fluoride ligands on an octahedron above, Ag1–F at 2.474(3) Å ($\times 2$), and once to an oxide

Table 3
Selected interatomic distances (Å) and angles (°) in $(Ag_3MoO_3F_3)(Ag_3MoO_4)Cl$

Atom 1	Atom 2	Mult.	Distance	Intra-polyhedral angles		Ideal angle
Mo1	O1	3 ×	1.769(6)			
	O3		1.79(1)			
				MoO_4^{2-} tetrahedron		
Mo2	F	3 ×	2.083(5)	O1–Mo1–O1	106.9(2)	109.5
	O2	3 ×	1.755(6)	O1–Mo1–O3	111.9(2)	109.5
Ag1	O1[a]	2 ×	2.447(4)	$MoO_3F_3^{3-}$ octahedron		
	O2		2.343(7)	F–Mo2–F	77.3(2)	90.0
	F	2 ×	2.474(3)	O2–Mo2–O2	103.1(3)	90.0
	Cl		2.717(3)	F–Mo2–O2	88.3(2)	90.0
				F–Mo2–O2	161.5(3)	180.0
Ag2	O1		2.395(7)			
	O2[a]	2 ×	2.558(4)			
	O3		2.353(5)			
	Cl		2.622(2)			

[a] An interchain distance.

ligand on an octahedron below, Ag1–O2 at 2.343(7) Å (× 2). The Ag–O distances between chains, marked with dashed lines in Fig. 1 and superscripts in Table 3, are longer than the Ag–O distances along the chains, compare Ag1–O1 with Ag1–O2 (2.447(4) Å vs. 2.343(7) Å) and also Ag2–O2 with Ag2–O1 (2.558(4) Å vs. 2.395(7) Å). Each Ag is also coordinated to one Cl^- ion, Ag1–Cl at 2.717(3) Å and Ag2–Cl at 2.622(2) Å.

3.2. Property measurements

Infrared measurements on $(Ag_3MoO_3F_3)(Ag_3MoO_4)Cl$ exhibit a very large peak at 830 cm^{-1}, with a shoulder (half the height) at ~800 cm^{-1}, within the range reported for Mo–O stretches [28,29]. These two absorption peaks correspond to the two sets of Mo–O distances in the compound, one set for $MoO_3F_3^{3-}$ and one set for MoO_4^{2-} (the four tetrahedral vertices have almost identical Mo–O distances). One small absorption peak was also present at 452 cm^{-1}, corresponding with that expected for Mo–F stretches [30]. No additional IR absorptions were detected in the 400–4000 cm^{-1} range, which is more typical for organic species. The Ag–(O/F/Cl) bond stretch frequencies are expected to come at much lower energies.

After diamagnetic corrections for the sample holder and atomic cores, $(Ag_3MoO_3F_3)(Ag_3MoO_4)Cl$ was appropriately diamagnetic, at -2.7×10^{-4} emu/mol with a small positive temperature dependence near ~25 K. The magnetic susceptibility is consistent with that expected for the closed shell metal ions Ag^+ and Mo^{6+} (d^0 configurations).

SHG measurements on an ungraded sample of $(Ag_3MoO_3F_3)(Ag_3MoO_4)Cl$ indicated an efficiency approximately 10 times that in α-quartz. However, the low SHG response may also reflect the racemically twinned nature of the crystals [8]. Higher SHG efficiencies are expected for non-racemically twinned crystals and for graded samples.

3.3. Dipole moments

In materials with polar chemical species, an individual dipole moment is typically partially or entirely (i.e., nonpolar) cancelled by neighboring dipole moments. The fact that the material crystallizes in a polar space group does not help quantify to what extent, or percent, the neighboring dipole moments counteract each other. As the $(Ag_3MoO_3F_3)(Ag_3MoO_4)Cl$ compound contains multiple polar anions, an analysis of the dipole moments seemed necessary to better understand the net dipole moment and the dipole–dipole interactions within the crystal packing. A simple bond-valence approach has been used to calculate the direction and magnitude of the $MoO_3F_3^{3-}$ and MoO_4^{2-} dipole moments, taking into account the non-ideal bond angles of both the octahedron and tetrahedron, respectively. This approach is analogous to that in the bond parameter technique, whereby individual bond polarizabilities, β_{ijk}, are vector-summed to determine the magnitude of the second-harmonic generation response $\langle d_{ijk}^{2\omega} \rangle$ [31,32].

The well-known Debye equation, $\mu = neR$ [33], (μ is the net dipole moment in Debye (10^{-18} esu cm), n the total number of electrons, e the charge on an electron, -4.8×10^{-10} esu, and R the difference, in cm, between the "centroids" of positive and negative charge) has been used to calculate the dipole moment of individual Mo–O and Mo–F bonds. Distribution of the electrons on the Mo/O/F atoms were estimated using bond-valence theory ($S_i = \exp[(R_o - R_i)/B]$; where R_o is an empirical constant, R_i is the length of the bond "i" in Å, and $B = 0.37$) [34]. We had previously applied these bond valence calculations to help us understand how to order the oxide-fluoride ligands, by estimating the charge on each of the ligands [35]. On the $MoO_3F_3^{3-}$ anion, the atomic valences were calculated to be Mo (+6), O (–1.51), and F (–0.48), to give dipole moments of 18.7 debye for Mo–O and 14.5 debye for Mo–F. A vector sum of the dipole moments for all six Mo–O/F bonds gives a net dipole moment of 6.1 debye, directed towards the fluoride face of the octahedron, yellow arrow in Fig. 3a. The direction of the dipole moment towards the less negative fluoride atoms may be somewhat surprising, but this is a result of the intraoctahedral distortion (i.e., the dipole moments to the fluoride atoms have a larger component along the c-axis). An identical calculation for the MoO_4^{2-} anion gave atomic valences for Mo (+5.75), O3 (−1.38), O1 (−1.46) and the calculated dipole moments of 18.2 debye for Mo–O3 and 17.9 debye for Mo–O1. Vector summation over the MoO_4^{2-} geometry gives a net dipole moment of 1.9 debye, much smaller than that for $MoO_3F_3^{3-}$, and is directed at the O1 'base' of the tetrahedron, yellow arrow in Fig. 3b. Two factors seem to control the magnitude of the dipole moments, (1) the amount of charge buildup on the O/F ligands and (2) the geometry of the anion. The former accounts for the larger Mo–O dipole moments compared to Mo–F, while the latter results in the larger net dipole moment for $MoO_3F_3^{3-}$ compared to MoO_4^{2-}. The Ag1 and Ag2 polyhedra (AgO_3F_2Cl and AgO_4F_2Cl, respectively) are also calculated to have a dipole moments directed down the negative c-axis of 4.5 and 2.9 debye, respectively, and also a component along the a-axis ($= b$) which self-cancels.

Dipole moments of both molybdenum anions align down the negative c-axis direction, and both fully contribute to the net dipole moment without any wasteful cancellation. Importantly, the complete alignment of dipole moments along the polar axis of a structure has been cited as the basis for highly efficient nonlinear optical materials, and has been given a

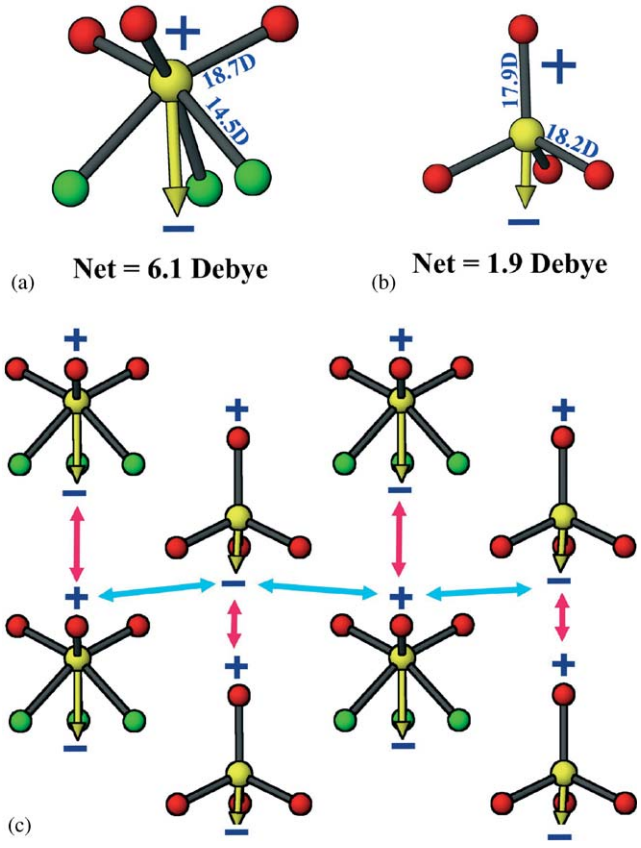

Fig. 3. Direction of the dipole moment vectors (yellow arrows) in a) the MoO_4^{2-} distorted tetrahedron and in b) the $MoO_3F_3^{3-}$ distorted octahedron. In the full crystal packing, c) the favorable dipole–dipole interactions are intrachain (light pink) and interchain (light blue).

structural parameter (*C*) [9]. Full crystal packing of the $MoO_3F_3^{3-}$ and MoO_4^{2-} anions, labeled with dipole vectors, is drawn in Fig. 3c. Favorable dipole-dipole interactions (+/−) occur between each $MoO_3F_3^{3-}$ and MoO_4^{2-} anion in the chain, and also between the two chains. Importantly, the offset of $\sim\frac{1}{2}\times c$ between neighboring chains helps align the favorable dipole-dipole interactions, as a result of the coordination by the Cl^- ion (described above). In the absence of Cl^-, i.e., no offset of $\sim\frac{1}{2}\times c$, unfavorable (+/+ or −/−) dipole–dipole interactions would occur. The oxide/fluoride ligand ordering, found here in $MoO_3F_3^{3-}$ for the first time, is attributable to the favorable dipole interactions both within the chain and between neighboring chains. Other relevant chain structures have disordered oxide–fluoride ligands, as in $CuW(py)_2(H_2O)_2O_2F_4$ or $CuNb(py)_4OF_5$ [36,37], and which apparently lack the favorable dipole–dipole interactions between neighboring chains. Suitable modification of the organic ligands may lead to more favorable dipole–dipole interactions.

Polar oxide–fluorides are excellent building blocks for noncentrosymmetric compounds, owing to their ability to mimic, and enhance, the intraoctahedral distortions

Table 4
Comparison of calculated dipole moments for selected polar octahedra

Compound	Species	Dipole moment[a] (debye units)	Distortion symmetry[b]
$Ag_6Mo_2ClO_7F_3$	MoO_3F_3	6.1	*C*3
KTiOPO4 [10]	TiO_6	4.5	*C*4
$LiNbO_3$ [9]	NbO_6	4.4	*C*3
$Cd(pyz)(H_2O)_2MoO_2F_4$ [8]	MoO_2F_4	2.3	*C*2
$BaTiO_3$ [38]	TiO_6	1.9	*C*2
$LiTaO_3$ [39]	TaO_6	1.8	*C*3

[a] Calculated according to the equation $\mu = neR$; μ is the dipole moment, n = total number of electrons, e = charge on the electron -4.8×10^{-10} esu, R = difference (in cm) between the center of mass of the protons and electrons; 1 debye unit = 10^{-18} esu cm (see text).

[b] The intraoctahedral distortion may conserve the *C*2, *C*3 or *C*4 rotation axes of an octahedron.

in the technologically useful $LiNbO_3$ and $KTiOPO_4$ (KTP) materials. To make this comparison clearer, dipole moments were calculated for these and a few relevant polar metal-oxide octahedra, Table 4. The polar distortion present in $MoO_3F_3^{3-}$ is indeed larger, by $\times 1.5$, than that for NbO_6 (in $LiNbO_3$) or TiO_6 (in KTP). Also, the dipole moment in the related $MoO_2F_4^{2-}$ anion is about four times weaker than in $MoO_3F_3^{3-}$, because the latter has a more asymmetrical ligand distribution down the polar axis. In idealized geometries, the dipole moments of metal oxide–fluorides would be expected to increase in the order $MOF_5 < MO_2F_4 < MO_3F_3$. However, the out-of-center metal displacements and the influence of different packing and bond networks are both reported to play a role in altering the metal polyhedra from their idealized geometries [40] (and as described above in the present compound), and it is difficult to predict which anion could potentially have the largest dipole moment within a particular structure type.

4. Conclusions

The $(Ag_3MoO_3F_3)(Ag_3MoO_4)Cl$ compound was synthesized via hydro(solvato)thermal methods and crystallizes in the polar space group *P*3*m*1. $(Ag_3MoO_3F_3)(Ag_3MoO_4)Cl$ comprises distorted, *fac*-$MoO_3F_3^{3-}$ octahedra and MoO_4^{2-} tetrahedra that are each connected through Ag^+ ions to neighboring polyhedra in a polar alignment down the *c*-axis. One Cl^- ion per formula unit serves to charge balance and offset the two types of chains by $\sim\frac{1}{2}\times c$. The title compound contains the first reported ordering of the oxide and fluoride ligands for $MoO_3F_3^{3-}$, and is described as owing to the inter- and intrachain dipole–dipole interactions. Dipole

moments for the $MoO_3F_3^{3-}$ and MoO_4^{2-} anions are both directed along the negative *c*-axis direction. The calculated dipole moment for the distorted $MoO_3F_3^{3-}$ anion is about $1.5\times$ larger than that for NbO_6 in $LiNbO_3$ or TiO_6 in KTP.

5. Supporting information

Further details of the crystal structure investigation can be obtained from the Fachinformationszentrum Karlsruhe, 76344 Eggenstein-Leopoldshafen, Germany, (fax: (49) 7247-808-666; e-mail: crysdata@fiz.karlsruhe.de) on quoting the depository number CSD 413082. An example calculation of the $MoO_3F_3^{3-}$ dipole moment is available from KRP.

Acknowledgments

The authors gratefully acknowledge support from the National Science Foundation (NSF), Solid State Chemistry, (Award No. DMR-9727516), and made use of the Central Facilities supported by the MRSEC program of the National Science Foundation (Grant DMR-0076097) at the Materials Research Center of Northwestern University. T.S.N. thanks the NSF for summer undergraduate research support as part of the REU program at Northwestern University. The authors also thank Professor Shiv Halasyamani for help with the SHG measurements, and also Professor George Schatz for helpful comments concerning the dipole moment calculations.

Note added in proof: Recent evidence for short range O/F ordering has been obtained from a combination of structured diffuse scattering and Monte Carlo modelling of $K_3MoO_3F_3$ [41].

References

[1] T. Hahn, International Tables for Crystallography, Vol. A. Kluwer Academic Publishers, Boston, USA, 2002, p. 805.
[2] P.S. Halasyamani, K.R. Poeppelmeier, Chem. Mater. 10 (1998) 2753.
[3] K.T. Holman, A.M. Pivovar, M.D. Ward, Science 294 (2001) 1907.
[4] W. Lin, O.R. Evans, R.-G. Xiong, Z. Wang, J. Am. Chem. Soc. 120 (1998) 13272.
[5] R.E. Sykora, K.M. Ok, P.S. Halasyamani, T.E. Albrecht-Schmitt, J. Am. Chem. Soc. 124 (2002) 1951.
[6] Y. Porter, K.M. Ok, N.S.P. Bhuvanesh, P.S. Halasyamani, Chem. Mater. 13 (2001) 1910.
[7] A.J. Norquist, K.R. Heier, P.S. Halasyamani, C.L. Stern, K.R. Poeppelmeier, Inorg. Chem. 40 (2001) 2015.
[8] P.A. Maggard, C.L. Stern, K.R. Poeppelmeier, J. Am. Chem. Soc. 123 (2001) 7742.
[9] N. Ye, Q. Chen, B. Wu, C. Chen, J. Appl. Phys. 84 (1998) 555.
[10] S.C. Abrahams, J.M. Reddy, J.L. Bernstein, J. Phys. Chem. Solids 27 (1966) 997.
[11] I. Trodjman, R. Masse, J.C. Guitel, Z. Krist. 139 (1974) 103.
[12] (a) M.E. Welk, A.J. Norquist, C.L. Stern, K.R. Poeppelmeier, Inorg. Chem. 40 (2001) 5479.
(b) M.E. Welk, A.J. Norquist, C.L. Stern, K.R. Poeppelmeier, Inorg. Chem. 39 (2000) 3946.
(c) K.R. Heier, A.J. Norquist, C.G. Wilson, C.L. Stern, K.R. Poeppelmeier, Inorg. Chem. 37 (1998) 76.
[13] L.J. Pauling, J. Am. Chem. Soc. 46 (1924) 2738.
[14] D. Babel, G. Pausewang, W. Viebahn, Z. Naturforsch. 22 (1967) 1219.
[15] O. Schmitz-Dumont, I. Heckmann, Z. Anorg. Allg. Chem. 267 (1952) 277.
[16] Z.G. Ye, J. Ravez, J.-P. Rivera, J.-P. Chaminade, H. Schmid, Ferroelectrics 124 (1991) 281.
[17] G. Pausewang, W. Ruedorff, Z. Anorg. Allg. Chem. 364 (1969) 69.
[18] S.C. Abrahams, J.L. Bernstein, J. Ravez, Acta Crystallogr. B 37 (1981) 1332.
[19] SAINTPLUS Bruker, AXS, Inc., Madison, WI, 1997.
[20] G.M. Sheldrick, SHELXTL Programs, Version 5.1 Bruker AXS, Inc., Madison, WI, 1998.
[21] A.L. Spek, PLATON, Utrecht University, Utrecht, The Netherlands, 2001.
[22] H.D. Flack, D. Schwarzenbach, Acta Crystallogr. A 44 (1988) 499–506.
[23] G.M. Sheldrick, Manual for SHELX-97, Universität Göttingen, Germany, 1997.
[24] H.D. Flack, G. Bernardinelli, J. Appl. Crystallogr. 33 (2000) 1143.
[25] H.D. Flack, G. Bernardinelli, Acta Crystallogr. A 55 (1999) 908.
[26] S.K. Kurtz, T.T. Perry, J. Appl. Phys. 39 (1968) 3798.
[27] R. Wang, H.D. Selby, H. Liu, M.D. Carducci, T. Jin, Z. Zheng, J.W. Anthis, R.J. Staples, Inorg. Chem. 41 (2002) 278.
[28] Y.Y. Kharitonov, Y.A. Buslaev, A.A. Kuznetsova, Z. Neorgan. Khim. 11 (1966) 821.
[29] G. Pausewang, R. Schmitt, K.Z. Dehicke, Z. Anorg. Allg. Chem. 408 (1974) 1.
[30] K. Nakamoto, Infrared and Raman Spectra of Inorganic and Coordination Compounds, Part A, Wiley, New York, NY, 1997.
[31] C.R. Jeggo, G.D. Boyd, J. Appl. Phys. 41 (1970) 2741.
[32] J. Goodey, J. Broussard, P. Shiv Halasyamani, Chem. Mater. 14 (2002) 3174.
[33] (a) P. Debye, Polar Molecules, Chemical Catalog Company, Inc., New York, NY, 1929.
(b) P. Debye, Phys. Z. 22 (1921) 302.
[34] I.D. Brown, D. Altermatt, Acta Crystallogr. B 41 (1985) 244.
[35] (a) A.J. Norquist, K.R. Heier, C.L. Stern, K.R. Poeppelmeier, Inorg. Chem. 37 (1998) 6495.
(b) A.J. Norquist, C.L. Stern, K.R. Poeppelmeier, Inorg. Chem. 38 (1998) 3448.
[36] P.S. Halasyamani, K.R. Heier, C.L. Stern, K.R. Poeppelmeier, Acta Crystallogr. C 53 (1997) 1240.
[37] P.S. Halasyamani, K.R. Heier, A.J. Norquist, C.L. Stern, K.R. Poeppelmeier, Inorg. Chem. 37 (1998) 369.
[38] G. Shirane, H. Danner, R. Pepinsky, Phys. Rev. 105 (1957) 856.
[39] S.C. Abrahams, J.L. Bernstein, J. Phys. Chem. Solids 28 (1967) 1685.
[40] M.E. Welk, A.J. Norquist, F.P. Arnold, C.L. Stern, K.R. Poeppelmeier, Inorg. Chem. 41 (2002) 5119.
[41] R.L. Withers, T.R. Welberry, F.J. Brink, L. Noren, J. Solid State Chem., in press.